Two-Step Transitions

DOI: 10.1002/anie.201005545

# A Symmetry-Breaking Spin-State Transition in Iron(III)**

*Michael Griffin, Stephen Shakespeare, Helena J. Shepherd, Charles J. Harding, Jean-François Létard, Cédric Desplanches, Andrés E. Goeta, Judith A. K. Howard, Annie K. Powell, Valeriu Mereacre, Yann Garcia, Anil D. Naik, Helge Müller-Bunz,* and Grace G. Morgan**

*In memory of Ian Hewitt*

Molecular spin crossover (SCO) has been intensively studied over the last 20 years, motivated both by the need to develop improved understanding of the phenomenon and in the hope of harnessing the switching for data storage and/or processing at the molecular level.[1] Development of increasingly sophisticated and imaginative methods of triggering and monitoring the effect,[2] and of clustering SCO centers into cooperative polymeric,[3] supramolecular,[4] or nanocrystalline[5] arrays, continues to fuel activity in this area.

Although the majority of spin-crossover (SCO) complexes exhibit a single magnetic transition between the high-spin (HS) and low-spin (LS) states, a number of examples of stepped crossover exist for $Fe^{II}$,[6–10] $Fe^{III}$[11] and $Co^{II}$.[12] In most examples this arises due to the presence of two well-defined lattice sites for mononuclear complexes, with different SCO transition temperatures for each site,[13] or, more rarely, in dinuclear complexes where each coordination site has a unique thermal response.[14]

In contrast to these examples, there has been a realization in recent years that spin crossover in mononuclear $Fe^{II}$ may be accompanied, or indeed triggered, by symmetry breaking in the crystal. In 2003 Bürgi et al. discovered that the two-step SCO in the well-studied complex $[Fe^{II}(2\text{-pic})_3]Cl_2\cdot EtOH$[15] (pic = 2-picolylamine) was accompanied by a crystallographic phase transition.[16] Here the single (HS) site at room temperature is replaced by a phase with two (HS, LS) iron sites in the intermediate region, before reverting to a phase with a single (LS) site at low temperature, which is isostructural with the HS regime. More recently, Collet and Tuchagues reported a beautiful example of a mononuclear $Fe^{II}$ complex with one light- and three thermally-induced crystallographic phases each accompanied by a spin-state change.[17] In this case the symmetry of the single (HS) site at room temperature is broken on cooling to a phase with two (HS, LS) sites at intermediate temperatures. Further cooling produces a third low temperature, LS phase, also with two (LS, LS) sites in a new space group, and irradiation of this phase at low temperature produces a spin transition and a fourth crystallographic phase with two independent HS sites, in an isomorphic subgroup of lower index than the original HS phase. A different but equally complicated phase diagram exists for the binuclear $Fe^{II}$ SCO complex with bridging 4,4′-bipyridine, terminal terpy-like and axial thiocyanate ligands.[18a] This was recently shown to have two distinct crystallographic phases within the first HS magnetic phase, onset of a third structural phase accompanying the thermal SCO to a $[HS{:}LS]_2$ regime which persists on photoswitching to a $[HS{:}HS]_2$ phase at low temperatures.[18b]

In contrast to these examples, Reedjik and Gamez have recently reported the $Fe^{II}$ complex $[Fe^{II}(L1)(SCN)_2]$ (see Figure 2 for L1) with a symmetry-breaking spin transition from a single HS site at high temperature to an intermediate phase (IP) with a HS:LS ratio of 1:2.[19] We now report the first example of concerted SCO and symmetry breaking in a $d^5$ ion, in the $Fe^{III}$ complex $[Fe^{III}(L2)]ClO_4$ (**1**) also with a 1:2 ratio of spin states in the IP, but in this case 1:2 LS:HS.

Magnetic data for **1** were collected between 10 and 300 K in both cooling and warming modes, and a plot of $\chi_M T$ versus temperature is shown in Figure 1. In the high-temperature regime (phase I), $\chi_M T$ has a value of 3.6 $cm^3 K mol^{-1}$ at 300 K

[*] Dr. M. Griffin, S. Shakespeare, Dr. H. Müller-Bunz, Dr. G. G. Morgan
The SFI-Strategic Research Cluster in Solar Energy Conversion
Centre for Synthesis and Chemical Biology
School of Chemistry and Chemical Biology
University College Dublin, Belfield, Dublin 4 (Ireland)
Fax: (+353) 1-716-2127
E-mail: grace.morgan@ucd.ie
helge.muellerbunz@ucd.ie
Dr. H. J. Shepherd,[+] Dr. A. E. Goeta, Prof. J. A. K. Howard
Department of Chemistry, University of Durham (UK)
Dr. J.-F. Létard, Dr. C. Desplanches
CNRS, Université de Bordeaux, ICMCB, Pessac (France)
Dr. C. J. Harding
Department of Chemistry, The Open University
Walton Hall (UK)
Prof. Dr. A. K. Powell, Dr. V. Mereacre
Institut für Anorganische Chemie
Karlsruhe Institut für Technologie (KIT) (Germany)
Prof. Dr. Y. Garcia, Dr. A. D. Naik
Institute of Condensed Matter and Nanosciences
Université Catholique de Louvain (Belgium)
[+] Present address: CNRS, Laboratoire de Chimie de Coordination (LCC), Toulouse (France)

[**] The authors thank Dr. Ivana R. Evans at the University of Durham for assistance with refining the unit cell parameters of the powder diffraction data and Prof. Sally Brooker and the University of Otago for funding and hosting a sabbatical visit (to G.G.M.) during manuscript preparation. Generous financial support from the Irish Research Council for Science, Technology and Engineering (IRCSET) and University College Dublin is also gratefully acknowledged, as is financial support from IAP-VI (P6/17) INANOMAT, the Fonds National de la Recherche Scientifique (FRFC 2.4508.08) and from a Concerted Research Action of the "Communauté Française de Belgique" allotted by the Académie Universitaire Louvain.

Supporting information for this article is available on the WWW under http://dx.doi.org/10.1002/anie.201005545.

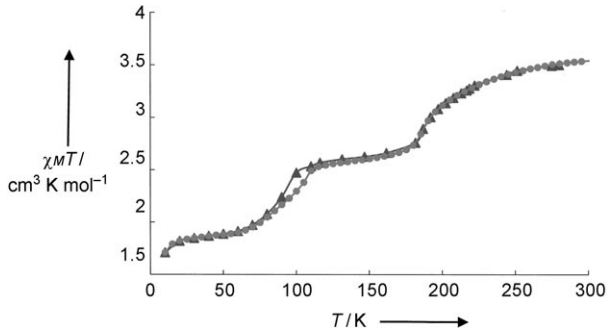


***Figure 1.*** Plot of $\chi_M T$ versus $T$ for **1**; ▲ = cooling mode, ● = warming mode.

asymptotic to about 3.8 $cm^3 K mol^{-1}$ or possibly higher. On cooling to 200 K, $\chi_M T$ falls to approximately 2.5–2.6 $cm^3 K mol^{-1}$, a value which persists to 100 K before undergoing a second, sharper transition to a value of approximately 1.9 $cm^3 K mol^{-1}$. On warming, a slight hysteresis is observed between 80–110 K around the transition between the low-temperature regime (phase III) and the IP (phase II), but no hysteresis is observed for the spin transition at 190 K. On cooling below 10 K, $\chi_M T$ reduces further, possibly due to zero-field splitting.

Crystallographic data for **1** were collected on a single crystal at multiple temperatures between 90 and 260 K. The structures recorded at 200 and 160 K are reported here.[20]

At 200 K the structure is very simple: the asymmetric unit comprises half a complex cation, Figure 2, and half a perchlorate anion, both on a twofold axis. The bond lengths

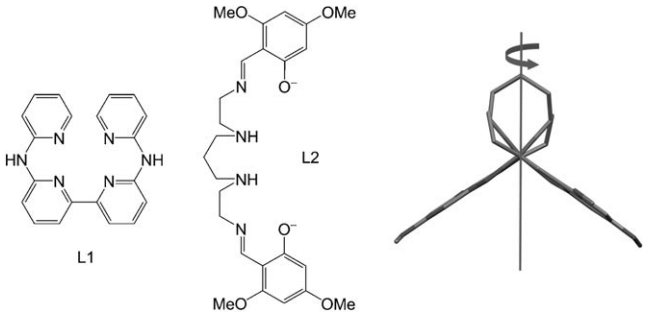


***Figure 2.*** View of L1, L2 and the cation of **1** showing the twofold axis in Phase II.

***Table 1:*** Bond lengths [Å] for **1** at 200 K (one site with $C_2$ axis) and at 160 K (two sites, one with internal $C_2$ axis).

| | 160 K | | 200 K |
|---|---|---|---|
| | Site 1 | Site 2 | Single site |
| | HS | LS | HS |
| | Occupancy = 1 | Occupancy = 0.5 | Occupancy = 0.5 |
| $Fe–O_{phen}$ | 1.915(3) | 1.871(3) | 1.906(2) |
| | 1.918(3) | | |
| $Fe–N_{imine}$ | 2.077(4) | 1.924(4) | 2.045(3) |
| | 2.088(4) | | |
| $Fe–N_{amine}$ | 2.185(4) | 2.002(4) | 2.144(3) |
| | 2.192(4) | | |

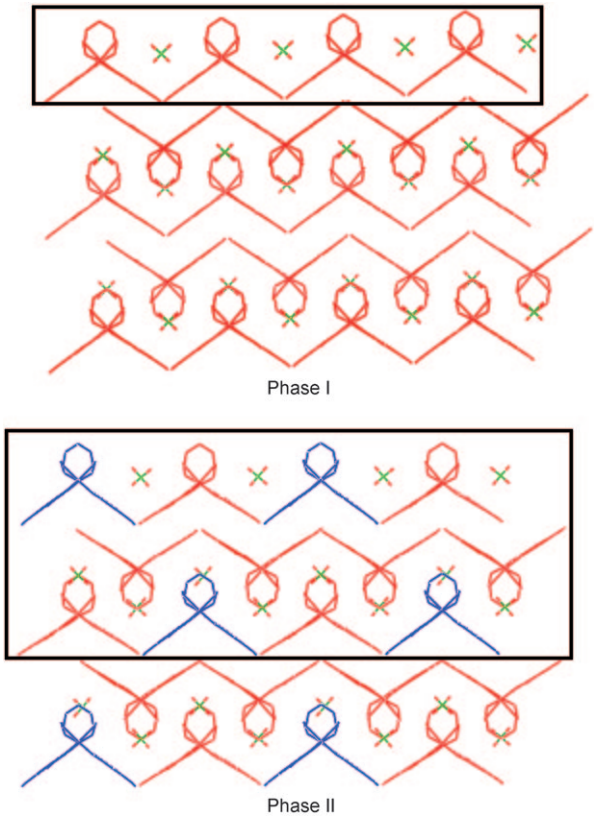


***Figure 3.*** Representation of unit cell contents within the crystal packing of **1** in structural and spin phases I and II. The boxes represent the relative contents of the unit cell in each case but do not represent the true unit cell. The unit cell contents viewed from different orientations are shown in the Supporting Information.

at 200 K (Table 1) are consistent with an $S = 5/2$ spin assignment clearly indicating HS $Fe^{III}$. Further cooling to 160 K at a rate of 1 $K min^{-1}$ triggered a phase transition, evidenced by the appearance of new superstructure reflections. The unit cell tripled and hence the asymmetric unit now contains one and a half complex molecules (Figure 3). The transition between phases I and II was clearly reversible and the crystal suffered no adverse effects after several cycles of data collections between 190 K and 220 K.

In the IP (100–200 K), the full occupancy cation has bond lengths and angles typical for HS $Fe^{III}$, whereas those in the half occupancy cation match those for the LS state (Table 1). For HS $Fe^{III}$ ions the spin-only value of $\chi_M T$ is 4.38 $cm^3 K mol^{-1}$, whereas it ranges from 0.5 to 0.7 $cm^3 K mol^{-1}$ for the LS ion.[13] Here one third of the cations are LS and two thirds are HS at intermediate temperature. The expected $\chi_M T$ calculated for one $Fe^{III}$ atom per formula is thus expected to be between $[4.38+4.38+0.5]/3 = 3.09$ and $[4.38+4.38+0.7]/3 = 3.15$ $cm^3 K mol^{-1}$.

On further cooling, the magnetic data clearly show a second spin transition of the same magnitude as the first indicating that a further one third of the cations have changed to LS. If two thirds of the sites are LS and one third is HS the

  

expected $\chi_M T$ would be between $[4.38+(2\times0.5)]/3 = 1.79$ and $[4.38+(2\times0.7)]/3 = 1.93\ cm^3\,K\,mol^{-1}$. This last value is in very good agreement with that observed at low temperatures. However at intermediate and room temperature the observed $\chi_M T$ is lower than expected for 100% spin conversion suggesting an incomplete LS→HS transition for the powdered sample used for the magnetic measurements, leading to a small LS fraction (ca. 20%) at high temperature.

Several attempts were made to collect single crystal data down to 30 K, but the quality of the crystal deteriorated to such an extent that it was not possible to index the diffraction pattern. However the unit cell parameters obtained from the single crystal experiments could be refined against the powder diffraction patterns obtained between 290 and 20 K[21] and the variation of the unit cell volume with temperature is shown in Figure 4. A pronounced discontinuity

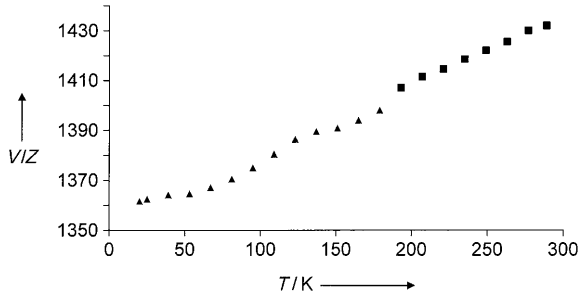


***Figure 4.*** Plot of normalized unit cell volume (*V*/*Z*) vs. temperature (*T*) between 290 and 20 K for **1**. The plot was obtained by refinement of the unit cell parameters (obtained from the single crystal data structures) against the powder diffraction data. The refined cell parameters were obtained from the phase I structure (■) and the phase II structure (▲) as appropriate.

in the thermal contraction of the unit cell is observed between 120 K and 80 K, which is in good agreement with the temperature of the second step of the spin transition determined from the SQUID measurement (Figure 1). This strongly suggests a second structural phase transition in this range of similar magnitude to that observed between phase I and phase II. The evidence for a structural contraction can be easily observed not only in the change in cell volume as a function of temperature, but also in the position of the Bragg peaks in the diffraction patterns themselves. On cooling it is usual that the positions of the diffraction peaks will move linearly to higher $2\theta$ values due to thermal contraction of the sample. The variable temperature diffraction experiment revealed two obvious discontinuities in this gradual shift in peak position at the temperatures corresponding to the steps of the spin transition (see Supporting Information).

One possibility to account for the onset of phase III is the existence of a crystallographic phase transition to a lower symmetry space group with an ordered distribution of HS sites in a predominantly LS lattice, resembling the infinite LS chains in the predominantly HS lattice observed in phase II. A second explanation could be that the phase III structure has the same space group and unit cell as phase II, but with HS sites located on the twofold axes. Two out of every three chains along the c-axis would be LS in this case, effectively the origin of the cell would shift relative to that of phase II. A third possibility is that no further crystallographic phase transition has taken place from phase II, with the additional LS molecules distributed randomly throughout the existing HS sites. This would result in an averaging of the bond lengths and angles for the fully occupied iron center to values which lie between the expected values for HS and LS molecules. However the presence of a slight hysteresis in the second partial SCO lends weight to the first two scenarios, as such hysteresis is often indicative of a crystallographic phase transition.

Thermodynamic parameters associated with the phase I–phase II spin transition were obtained by differential scanning calorimetry over the temperature range 98–300 K at several scanning rates. The best data were obtained at $10\ K\,min^{-1}$ where on warming from 98 K, a peak characteristic of a first order phase transition was observed at $T_{max} = 200(5)$ K coinciding with the temperature of the magnetic and structural transition (Supporting Information, Figure S12). On cooling a similar peak was observed thus confirming the absence of a hysteresis effect at this temperature. The enthalpy and entropy values were evaluated as $\Delta H = 7.88\ kJ\,mol^{-1}$ and $\Delta S = 39.4\ J\,mol^{-1}\,K^{-1}$ for the first step of the spin conversion profile. The entropy change at this temperature is much higher than that expected if only an electronic contribution is considered ($\Delta S_{el} = 9.13\ J\,mol^{-1}\,K^{-1}$) thereby permitting derivation of the vibrational entropy associated with the spin conversion at this step as $\Delta S_{vib} = 30.27\ J\,mol^{-1}\,K^{-1}$. Although it was not possible to calculate the total entropy due to inaccessibility of the low temperature profile with our experimental setup, this large vibrational entropy value suggests a large modification of vibrations at 200 K in line with the crystallographic data.

At 20 and 50 K the Mössbauer spectra for **1** (Figure 5 and Table S5, Figures S13–15) represent an overlap of a strongly asymmetric LS quadrupole doublet with an isomer shift of $\delta = 0.216(1)\ mm\,s^{-1}$ (relative to α-Fe) and a quadrupole splitting of $3.06\ mm\,s^{-1}$, which is typical for $Fe^{III}$ ions in the LS state, and an extremely broad singlet with an isomer shift $\delta = 0.50(1)\ mm\,s^{-1}$ typical for $Fe^{III}$ ions in the HS state.

The ratios of the peak areas for HS and LS species are 39.7:60.3 and 39.1:60.9 at 20 and 50 K, respectively. According to the susceptibility data at these temperatures the HS:LS ratio should be 33.3:66.6. The deviation of the area ratio for HS and LS is caused by the different Lamb–Mössbauer factors for each species. Above 50 K, the HS singlet increases in intensity and the LS doublet decreases in intensity with increasing temperature. The ratios of the peak areas for HS and LS doublets becomes 64.2:35.8 at 175 K, which unambiguously indicates the occurrence of transition between the low temperature 1:2 HS:LS ratio to intermediate temperature 2:1 HS:LS ratio. The Mössbauer spectrum at 280 K is in the form of a broad singlet, which might also be considered as a very broad and asymmetric doublet with small quadrupole splitting, and suggests the occurrence of a complete spin conversion at this temperature. Mössbauer and magnetic susceptibility data both converge to an assignment of a 2:1

  

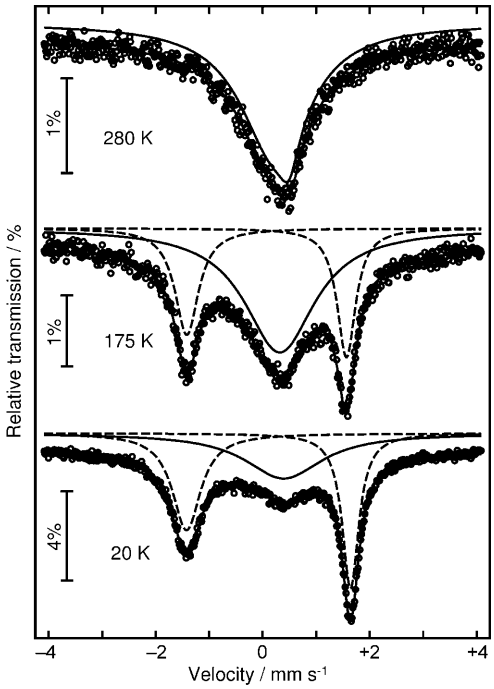


***Figure 5.*** Variable-temperature $^{57}$Fe Mössbauer spectra of **1**.

HS:LS ratio in phase II which shifts to a 1:2 HS:LS ratio in phase III (Figure S15).

Of equal importance to discovering the nature of phase III is determining why and how the ordered IP forms. For $[Fe^{II}(L1)(NCS)_2]$, it was suggested that onset of an IP with an ordered array of HS and LS centers in the unusual ratio of 1:2 might be because 100% conversion from HS to LS states in one step was energetically too unfavorable given the considerable structural changes involved.[19,22] This suggests that the origin of the stepped SCO in that species could be structural rather than a result of short range interactions. In **1** the structural modification during the first phase transition is identical on a molecular level to that observed in $[Fe^{II}(L1)(NCS)_2]$. In both cases the molecules in the HS phase all have $C_2$ symmetry and in the IP only one of the two crystallographically independent molecules possesses this site symmetry. In **1** the number of molecules in the asymmetric unit increases from a half to one and a half creating a supercell with three times the volume of the high temperature phase. Consequently, it is possible that the stepped nature of the spin transition in **1** may also be attributable to the structural rearrangement, rather than as a direct result of the magnetic interactions within the structure.

However, in $[Fe^{II}(2\text{-pic})_3]Cl_2{\cdot}EtOH$ it was suggested that the ordered intermediate state is the result of competitive effects between local short-range interactions between dimers and long-range elastic interactions.[16a] Long-range elastic interactions depend upon strong intermolecular contacts to communicate the spin transition to all $Fe^{II}$ centers in the lattice.[23] Ferric cations such as $[Fe^{III}(L2)]^+$ generally show poor cooperativity unless very strong intermolecular interactions are present in the lattice. In this sample, no strong intermolecular interactions are apparent and therefore long-range elastic interactions should be very weak or non-existent. The origin of the concerted structural and spin transitions may therefore be primarily driven by structural constraints, which preclude total conversion to LS in one step as suggested for $[Fe^{II}(L1)(NCS)_2]$ as the lattice strain would be too severe.[19,22] Solid-state DFT calculations are currently underway to determine the influence of the lattice on the stepped spin transition and to try to elucidate if the crystallographic symmetry breaking is indeed independent of any symmetry-breaking magnetic interaction.[24]

To conclude, $[Fe^{III}(L2)]ClO_4$ represents the first example of concerted SCO and symmetry breaking in a $d^5$ ion. Work is currently underway to fully explore the interplay between the structural and spin transitions in this complex using Raman spectroscopy and solid-state DFT calculations, in the quest to further understand how changing the local electronic state affects the crystal symmetry in this and other stepped SCO systems.

## *Experimental Section*

*N,N'*-bis(2-aminoethyl)-1,3-propanediamine (0.160 g, 1 mmol) and 4,6-dimethoxysalicylaldehyde (0.364 g, 2 mmol) were dissolved in methanol (15 mL) producing a bright yellow solution. This was stirred for 1 h at room temperature. Iron(III) perchlorate hydrate (0.354 g, 1 mmol) dissolved in methanol (15 mL) was then filtered into the yellow solution resulting in a dark purple solution. After 10 min stirring the solution was filtered and a dark purple/brown powder was collected which was recrystallized from acetone:ethanol (1:1) solution. After a day this solution was again filtered and a brown powder was collected (0.304 g, 53.4%). After a further day the filtrate was filtered again and dark purple crystals were collected (0.165 g, 25.8%). Elemental analysis (%): $[Fe(L2)]ClO_4$, **1**: calcd for $C_{25}H_{34}Cl\,FeN_4O_{10}$: C 46.85, H 5.35, N, 8.74; found C 46.60, H 5.32, N 8.58. Magnetic susceptibility was measured between 4 and 300 K on an MPMS-5T Quantum Design SQUID magnetometer. Experimental susceptibilities were corrected for diamagnetism of the constituent atoms using Pascal's constants. Single-crystal X-ray diffraction experiments were carried out on a SMART 3-circle diffractometer with a 6 K CCD area detector, using graphite-monochromated $Mo_{K\alpha}$ radiation ($\lambda = 0.71073$ Å) and an open-flow $N_2$ Cryostream (Oxford Cryosystems). The structures were solved by Direct Methods using SHELXS, and refined by full-matrix least-squares on $F^2$ using SHELXL-97[26] and the graphical user interface Olex2.[26] Full data collections were performed at 200 K and 160 K. Several attempts were made to collect single crystal data down to 30 K (using the Oxford Cryosystems Helix to control the temperature), but the crystal disintegrated during further cooling from 115 K, to such an extent that the pattern could not be indexed.

Variable temperature powder X-ray diffraction data were collected using a Bruker AXS D8 Advance diffractometer and temperature was controlled with an Oxford Cryosystems PheniX helium cryostat. The sample was cooled at a rate of 12 K h$^{-1}$ from 290 K to 20 K while collecting data in the $2\theta$ range 5–35° in 0.05° steps, using a counting time of 0.3 s per step. Structural figures were generated using Mercury.[27]

Received: September 4, 2010
Published online: November 12, 2010

**Keywords:** iron · magnetism · phase transitions · spin crossover · symmetry breaking

  

[1] a) P. Gütlich, H. A. Goodwin, *Top. Curr. Chem.* **2004**, *233*, 1 – 47; b) J. F. Létard, P. Guionneau, L. Goux-Capes, *Top. Curr. Chem.* **2004**, *235*, 221 – 249.

[2] S. Bonhommeau, G. Molnár, A. Galet, A. Zwick, J.- A. Real, J. J. McGarvey, A. Bousseksou, *Angew. Chem.* **2005**, *117*, 4137 – 4141; *Angew. Chem. Int. Ed.* **2005**, *44*, 4069 – 4073.

[3] V. Niel, A. L. Thompson, M. C. Muñoz, A. Galet, A. E. Goeta, J. A. Real, *Angew. Chem.* **2003**, *115*, 3890 – 3893; *Angew. Chem. Int. Ed.* **2003**, *42*, 3760 – 3763; V. Niel, J. M. Martínez-Agudo, M. C. Muñoz, A. B. Gaspar, J. A. Real, *Inorg. Chem.* **2001**, *40*, 3838 – 3839.

[4] a) C. Gandolfi, C. Moitzi, P. Schurtenberger, G. G. Morgan, M. Albrecht, *J. Am. Chem. Soc.* **2008**, *130*, 14434 – 14435; b) P. N. Martinho, C. J. Harding, H. Müller-Bunz, M. Albrecht, G. G. Morgan, *Eur. J. Inorg. Chem.* **2010**, 675 – 679.

[5] a) M. Cavallini, I. Bergenti, S. Milita, G. Ruani, Salitros, Z.-R. Qu, R. Chandrasekar, M. Ruben, *Angew. Chem.* **2008**, *120*, 8724 – 8728; *Angew. Chem. Int. Ed.* **2008**, *47*, 8596 – 8600; b) I. Boldog, A. B. Gaspar, V. Martínez, P. Pardo-Ibañez, V. Ksenofontov, A. Bhattacharjee, P. Gütlich, J. A. Real, *Angew. Chem.* **2008**, *120*, 6533 – 6537; *Angew. Chem. Int. Ed.* **2008**, *47*, 6433 – 6437; c) F. Volatron, L. Catala, E. Rivière, A. Gloter, O. Stéphan, T. Mallah, *Inorg. Chem.* **2008**, *47*, 6584 – 6586; d) T. Forestier, S. Mornet, N. Daro, T. Nishihara, S.-I. Mouri, K. Tanaka, O. Fouché, E. Freysz, J.-F. Létard, *Chem. Commun.* **2008**, 4327 – 4329; e) T. Forestier, A. Kaiba, S. Pechev, D. Denux, P. Guionneau, C. Etrillard, N. Daro, E. Freysz, J.-F. Létard, *Chem. Eur. J.* **2009**, *15*, 6122 – 6130.

[6] H. Köppen, E. W. Müller, C. P. Köhler, H. Spiering, E. Meissner, P. Gütlich, *Chem. Phys. Lett.* **1982**, *91*, 348 – 352.

[7] Y. Garcia, O. Kahn, L. Rabardel, B. Chansou, L. Salmon, J. P. Tuchagues, *Inorg. Chem.* **1999**, *38*, 4663 – 4670.

[8] D. Boinnard, A. Bousseksou, A. Dworkin, J. M. Savariault, F. Varret, J. P. Tuchagues, *Inorg. Chem.* **1994**, *33*, 271 – 281.

[9] D. L. Reger, C. A. Little, V. G. Young, M. Pink, *Inorg. Chem.* **2001**, *40*, 2870 – 2874.

[10] C. F. Sheu, S. Pillet, Y. C. Lin, S. M. Chen, I. J. Hsu, C. Lecomte, Y. Wang, *Inorg. Chem.* **2008**, *47*, 10866 – 10874.

[11] a) J. Tang, J. Sanchez Costa, S. Smulders, G. Molnar, A. Bousseksou, S. J. Teat, Y. Li, G. A. vanAlbada, P. Gamez, J. Reedjik, *Inorg. Chem.* **2009**, *48*, 2128 – 2135; b) M. S. Shongwe, B. A. Al-Rashdi, H. Adams, M. J. Morris, M. Mikuriya, G. R. Hearne, *Inorg. Chem.* **2007**, *46*, 9558 – 9568.

[12] R. Clérac, F. A. Cotton, K. R. Dunbar, T. Lu, C. A. Murillo, X. Wang, *J. Am. Chem. Soc.* **2000**, *122*, 2272 – 2278.

[13] O. Kahn, *Molecular Magnetism*, Wiley-VCH, Weinheim, **1993**, p. 10.

[14] a) J. A. Real, H. Bolvin, A. Bousseksou, A. Dworkin, O. Kahn, F. Varret, J. Zarembowitch, *J. Am. Chem. Soc.* **1992**, *114*, 4650 – 4658; b) A. B. Gaspar, V. Ksenofontov, S. Reiman, P. Gütlich, A. L. Thompson, A. Goeta, M. Carmen Muñoz, J. A. Real, *Chem. Eur. J.* **2006**, *12*, 9289; c) M. H. Klingele, B. Moubaraki, J. D. Cashion, K. S. Murray, S. Brooker, *Chem. Commun.* **2005**, 987 – 989.

[15] a) L. Wiehl, G. Kiel, C. P. Köhler, H. Spiering, P. Gütlich, *Inorg. Chem.* **1986**, *25*, 1565 – 1571; b) R. Jakobi, H. Spiering, P. Gütlich, *J. Phys. Chem. Solids* **1992**, *53*, 267 – 275; c) P. Gütlich, A. Hauser, H. Spiering, *Angew. Chem.* **1994**, *106*, 2109 – 2141; *Angew. Chem. Int. Ed. Engl.* **1994**, *33*, 2024 – 2054; d) H. Romstedt, A. Hauser, H. Spiering, *J. Phys. Chem. Solids* **1998**, *59*, 265 – 275.

[16] a) D. Chernyshov, M. Hostettler, K. W. Törnroos, H. B. Bürgi, *Angew. Chem.* **2003**, *115*, 3955 – 3960; *Angew. Chem. Int. Ed.* **2003**, *42*, 3825 – 3830; b) M. Hostettler, K. W. Törnroos, D. Chernyshov, B. Vangdal, H. B. Bürgi, *Angew. Chem.* **2004**, *116*, 4689 – 4695; *Angew. Chem. Int. Ed.* **2004**, *43*, 4589 – 4594; c) K. W. Törnroos, M. Hostettler, D. Chernyshov, B. Vangdal, H. B. Bürgi, *Chem. Eur. J.* **2006**, *12*, 6207 – 6215.

[17] N. Bréfuel, H. Watanabe, L. Toupet, J. Come, N. Matsumoto, E. Collet, K. Tanaka, J. P. Tuchagues, *Angew. Chem.* **2009**, *121*, 9468 – 9471; *Angew. Chem. Int. Ed.* **2009**, *48*, 9304 – 9307.

[18] a) D. Fedaoui, Y. Bouhadja, A. Kaiba, P. Guionneau, J.-F. Létard, P. Rosa, *Eur. J. Inorg. Chem.* **2008**, 1022 – 1026; b) A. Kaiba, H. J. Shepherd, D. Fedaoui, P. Rosa, A. E. Goeta, N. Rebbani, J. F. Létard, P. Guionneau, *Dalton Trans.* **2010**, *39*, 2910 – 2918.

[19] S. Bonnet, M. A. Siegler, J. S. Costa, G. Molnár, A. Bousseksou, A. L. Spek, P. Gamez, J. Reedjik, *Chem. Commun.* **2008**, 5619 – 5621.

[20] 200 K: monoclinic; space group $C2/c$; $a = 10.040(1)$, $b = 25.038(4)$, $c = 11.634(2)$ Å, $\beta = 103.164(2)°$, $V = 2847.7(7)$ Å$^3$; $\rho_{calcd} = 1.133$ Mg m$^{-3}$; $2\Theta_{max} = 52.86°$; $Mo_{K\alpha}$ radiation ($\lambda = 0.71073$ Å); $\phi$-$\omega$-scans; 12293 reflections collected, 2758 unique (all included in refinement); correction for Lorentzian polarization and absorption: semi-empirical from equivalents (program SADABS;[25] $\mu = 0.568$ mm$^{-1}$, max. and min. transmission 0.899 and 0.801); 346 parameters; hydrogen atoms were refined freely; $R1 = 0.064$, $wR2 = 0.119$ (all data); residual electron density: 0.431/−0.313 e$^-$ Å$^{-3}$. 160 K: monoclinic; $C2/c$; $a = 23.1785(6)$, $b = 24.7163(9)$, $c = 16.9116(6)$ Å, $\beta = 120.487(2)°$, $V = 8348.9(5)$ Å$^3$; $\rho_{calcd} = 1.532$ Mg m$^{-3}$; $2\theta_{max} = 50.00°$; $Mo_{K\alpha}$ radiation ($\lambda = 0.71073$ Å); $\phi$-$\omega$-scans; 52322 reflections collected, 7382 unique (all included in refinement); correction for Lorentzian polarization and absorption: semi-empirical from equivalents (program SADABS;[25] $\mu = 0.702$ mm$^{-1}$, max. and min. transmission 0.899 and 0.824); 572 parameters; hydrogen atoms were added at calculated positions; $R1 = 0.113$, $wR2 = 0.1722$ (all data); residual electron density: 0.909/−1.213 e$^-$ Å$^{-3}$. CCDC 773987 (200 K) and 773988 (160 K) contain the supplementary crystallographic data for this paper. These data can be obtained free of charge from The Cambridge Crystallographic Data Centre via www.ccdc.cam.ac.uk/data_request/cif.

[21] Topas Academic (http://www.topas-academic.net/) was used to refine the powder diffraction data (obtained from single-crystal diffraction experiments) between 290 and 20 K. The structural parameters refined were the cell parameters, an overall isotropic temperature factor, sample displacement, eighteen background terms and five peak shape function terms. Further details are listed in the Supporting Information.

[22] S. Bonnet, G. Molnár, J. S. Costa, M. A. Siegler, A. L. Spek, A. Bousseksou, W.-T. Fu, P. Gamez, J. Reedjik, *Chem. Mater.* **2009**, *21*, 1123 – 1136.

[23] a) A. Bousseksou, J. Nasser, J. Linares, K. Boukheddaden, F. Varret, *J. Phys.* **1992**, *2*, 1381 – 1403; b) H. Bolvin, *Chem. Phys.* **1996**, *211*, 101 – 114; c) J. A. Real, A. B. Gaspar, V. Niel, M. C. Muñoz, *Coord. Chem. Rev.* **2003**, *236*, 121 – 141.

[24] A. Bousseksou, F. Varret, J. Nasser, *J. Phys. I* **1993**, *3*, 1463 – 1473.

[25] G. M. Sheldrick, *Acta Crystallogr. Sect. A* **2008**, *64*, 112 – 122.

[26] O. V. Dolomanov, L. J. Bourhis, R. J. Gildea, J. A. K. Howard, H. Puschmann, *J. Appl. Crystallogr.* **2009**, *42*, 339 – 341.

[27] I. J. Bruno, J. C. Cole, P. R. Edgington, M. K. Kessler, C. F. Macrae, P. McCabe, J. Pearson, R. Taylor, *Acta Crystallogr. Sect. B* **2002**, *58*, 389 – 397.


  